

Resistance of through-thickness grain boundaries to cleavage cracking in silicon thin films

Yu Qiao* and Jin Chen

Department of Structural Engineering, University of California – San Diego La Jolla, CA 92093-0085, USA

Received 31 January 2008; revised 3 March 2008; accepted 18 March 2008
Available online 28 March 2008

Through a set of microtensile experiments, it was discovered that the resistance of a free-standing polycrystalline silicon thin film to cleavage cracking is not a material constant. Rather, it is highly dependent on the film thickness. As the film thickness changes from 1 to 10 μm , the fracture resistance increases by 20–60%, which can be attributed to the nonuniform nature of the crack front advance across grain boundaries.

© 2008 Published by Elsevier Ltd. on behalf of Acta Materialia Inc.

Keywords: Thin films; Fracture; Grain boundaries; Toughness

With the development of processing techniques of semiconductors, such as silicon and germanium, their reliability under tensile stresses or impact loadings has become increasingly important [1,2]. Most semiconductors are intrinsically brittle [3–5]. When the temperature is relatively low, dislocations may be nucleated, but the initiation and development of double kinks can be difficult, i.e. the dislocations tend to be immobile [6,7]. Consequently, the strain energy in a crack-tip zone cannot be dissipated by plastic deformation, and the fracture toughness is governed by the resistance to cleavage cracking. Over the years, a large number of experimental studies have been carried out on fracture behaviors of thin-film polycrystalline silicon, since it is one of the most widely used materials for microelectromechanical systems (MEMS) and integrated circuits. During processing and service, unexpected failures have frequently been reported. Through microtensile and microcantilever experiments on smooth-bar-type samples [8–14], the critical stress intensity factor of polysilicon was determined to be 1–2 $\text{MPa m}^{1/2}$. However, the data scatter was large, because the details of crystalline structures were usually not taken into account [15–18]. For instance, it was noticed that if the crack tip was arrested by a grain boundary, the measured toughness would be higher [19].

The barrier effect of grain boundaries on cleavage crack propagation has been reported over many years. Microcracks produced during manufacturing and handling are often grain-sized. Thus, in many cases, the fracture resistance of a brittle material is dominated by the grain boundary toughness, instead of the fracture resistance of crystallographic planes [20]. The breakthrough of a microcrack across a few grain boundaries could lead to catastrophic failure [21–23]. Recently, through a bicrystal fracture experiment [24,25], it was confirmed that grain boundary toughness is dominated by crystallographic misorientations, particularly twist and tilt angles. As a cleavage front encounters a grain boundary, the front would first penetrate through the boundary at a series of breakthrough points (BTPs), somewhat similar to a dislocation line bypassing an array of precipitates, which leads to the formation of regular river markings. The persistent grain boundary islands (PGBIs) between the BTPs will not be separated until the critical penetration depth of the crack front is reached.

In a thin film material, since grains of unfavorable orientations are buried during the film growth process, grain boundaries tend to be through-thickness [26]. When the film thickness is less than the distance between adjacent river markings, there would be only a single BTP along the crack front. Under this condition, if the film thickness varies, the area of PGBI would change, and therefore the grain boundary toughness may be different [27]. That is, the boundary toughness is no longer a material constant. Note that this size effect is intrinsic,

* Corresponding author. Tel.: +1 858 534 3388; e-mail: yqiao@ucsd.edu

and entirely different from the weakest link effect [28], which is less pronounced when the characteristic length scale and defect density are small.

In the current study, a boron-doped polycrystalline silicon was investigated. The as-received material was in wafer form, with a thickness of 4 mm and a diameter of 200 mm. The resistivity was 0.55 Ω cm. The grain size was in the range of 5–15 μ m. The silicon wafer was heated in a tube furnace at 450 $^{\circ}$ C for 0.5 h, followed by partial quenching in cold water, by which a large number of thermal cracks were produced. Under a XTL-VI stereo trinocular microscope, the cracks arrested by through-thickness grain boundaries were identified, and 15 \times 15 mm rectangle pieces surrounding the crack tips were harvested and sliced into 200 μ m thick films by electrical discharge machining. In each group of pre-cracked films, the cracks were in grains of identical crystallographic orientations.

The films were cleaned in a mixture of four parts of 98% sulfuric acid and one part of 30% hydrogen peroxide at 90 $^{\circ}$ C for 15 min, rinsed in deionized water and slightly etched for 10 min. The etchant comprised of 7% hydrofluoric acid, 75% nitric acid, and 18% acetic acid. After rinsing in ethanol, the films were dried in a vacuum furnace at 100 $^{\circ}$ C for 30 min, then modified in a 20% toluene solution of chlorotrimethylsilane at 90 $^{\circ}$ C for 5 days, so that the pre-crack surfaces as well as the film surfaces were covered by a dense layer of hydrophobic silane groups. The surface-treated films were mechanically polished to about 150 μ m thick, and finally thinned to 1–30 μ m through chemical etching in the hydrofluoric acid etchant. Films thicker than 100 μ m were not investigated in the current study. During etching, the sample was placed in a porous Teflon container and the etchant was driven by an Omega FPU-500 peristaltic pump to flow across the sample surface at a constant rate of 30 ml min⁻¹. The etching rate was 3–5 μ m min⁻¹. Prior to the tensile test, the samples were heat treated at 350 $^{\circ}$ C in vacuum for 12 h and thoroughly cleaned in acetone and ethanol. The pre-crack length (\sim 0.5 mm) was measured through the stereomicroscope.

The thin film samples were then mounted on a micro-testing machine, with both ends fixed on testing stages by Loctite-411 glue. The details of the microtensile testing machine have been described elsewhere [29]. The machine was capable of applying a tensile load at a rate of 10 μ m s⁻¹, with resolutions of load and displacement of 0.3 μ N and 20 nm, respectively. The fracture surfaces were observed in a FEI XL30 environmental scanning electron microscope, as shown in Figures 1 and 2. Using the measured peak load of grain boundary failure, F_p , the boundary toughness was calculated in the framework of linear elastic fracture mechanics [30], $K_{gb} = (F_p/wt)\sqrt{\pi a} \cdot f$, where w and t are the width and the thickness of the thin film sample, respectively, a is the pre-crack length and $f = 1.12 - 1.39(a/w) + 7.3(a/w)^2 - 13(a/w)^3 + 14(a/w)^4$ is the geometry factor. The results are shown in Figure 3.

When the film thickness is relatively large, e.g. when $t > 20$ μ m, the cleavage front would break through the boundary at multiple locations simultaneously (Figure 1). At each BTP, the front first penetrates

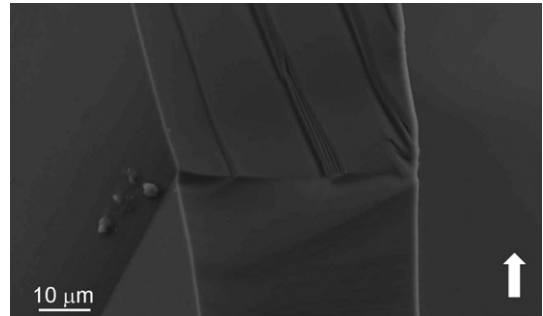


Figure 1. Cleavage cracking across a through-thickness grain boundary in a thick film sample. The arrow indicates the crack propagation direction.

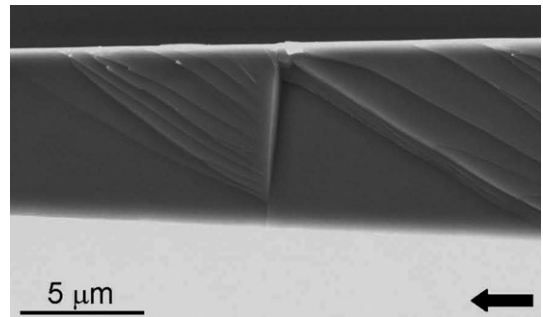


Figure 2. Cleavage cracking across a through-thickness grain boundary in a thin film sample. The arrow indicates the crack propagation direction.

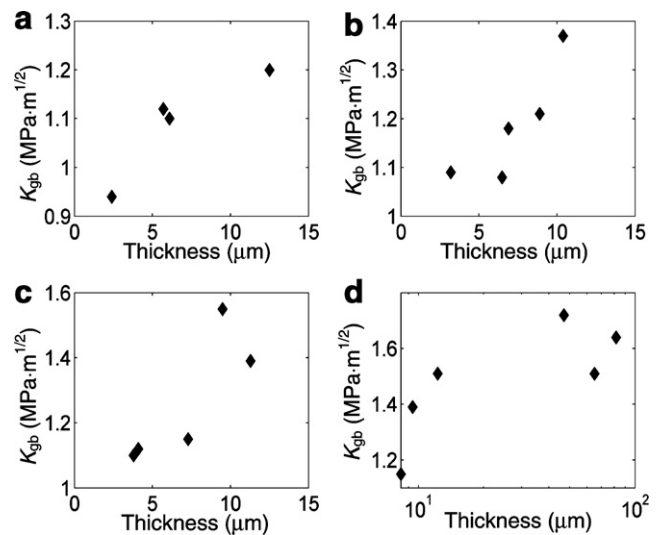


Figure 3. The measured grain boundary toughness, K_{gb} , as a function of the film thickness, t . (a) Group 1 samples, with twist (θ) and tilt (ϕ) angles of 4.3 $^{\circ}$ and 5.6 $^{\circ}$, respectively; (b) group 2 samples ($\theta = 11.1^{\circ}$, $\phi = 4.2^{\circ}$); (c) group 3 samples ($\theta = 7.6^{\circ}$, $\phi = 12.4^{\circ}$); and (d) group 4 samples ($\theta = 9.1^{\circ}$, $\phi = 17.2^{\circ}$).

through the boundary quasi-stably, with the remainder being arrested by the grain boundary. The characteristic distance between adjacent BTPs, D , is in the range of 5–10 μ m. The PGBIs are formed geometrically necessarily, since the fracture surfaces must shift from the cleavage plane of the grain behind the boundary (“B”) to that of the grain ahead of the boundary (“A”). As the front

penetration depth keeps increasing, eventually the PGIBs are separated by either shear fracture or shear yielding [25]. The terrains in grain “A” are connected via secondary cracking, which leads to the formation of cleavage ridges. On the one hand, if the BTPs are far apart, the PGIB area would be large, and separation would require a large amount of work. Before the local crack-tip stress can increase to a high level, new BTPs would develop in between the existing ones, and thus D would decrease. On the other hand, if D is too small, while the PGIB area would be minimized, the surface roughness in grain “A” associated with the formation of cleavage ridges would increase. In these areas, crack front advance is difficult; that is, some of the BTPs would be deactivated, which would effectively cause D to increase. As the two competing mechanisms are in balance, the optimum BTP distance is reached and the resistance of grain boundaries to cleavage cracking is minimized [31].

The cleavage plane in silicon can be either $\{111\}$ or $\{110\}$. The fracture toughness of them differ by 5% [32], which is within the tolerance of the testing system. Thus, it will not be taken into consideration in the following discussion. Because of the relatively large number of possible cleavage planes, the twist and tilt misorientation angles across a boundary in silicon are usually smaller than 15° [33]. The twist angle, θ , is more important compared with the tilt angle, ϕ , and their effects can be collectively described by [24]

$$G = (\sin \theta + \cos \theta) / \cos^2 \phi + C \cdot \sin \theta \cos \theta / \cos \phi \quad (1)$$

where G is the normalized fracture resistance and C is a material parameter. Under this condition, since the BTPs distribute along the boundary quasi-periodically, the grain boundary toughness is determined by the averaged effects of them. Consequently, for a thick film, K_{gb} is quite independent of the film thickness, t .

In a thin film sample ($t < 15 \mu\text{m}$), the boundary width is insufficient for multiple BTPs (Fig. 2), where only a single BTP can be formed. This process is also depicted in Figure 4. Initially, the crack tip is arrested by the

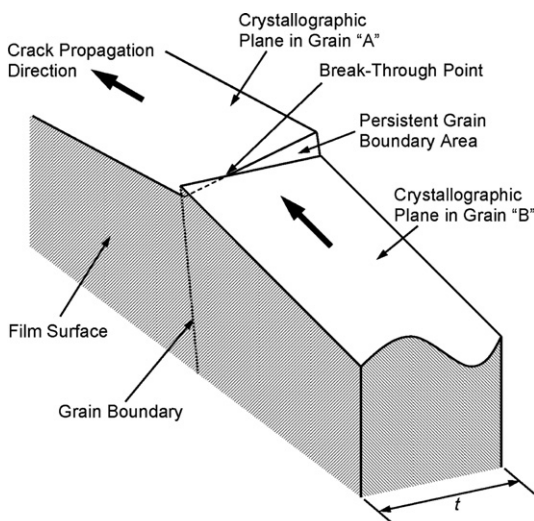


Figure 4. Schematic of a cleavage crack propagating through a through-thickness grain boundary in a free-standing thin film.

grain boundary. As the crack-tip stress intensity rises, the cleavage front penetrates through the boundary at the point where the local stress intensity is relatively high and the local fracture resistance is relatively low [24]. While there may be more than one suitable site for the front penetration, only one of them can be active; otherwise the increase in the crack growth driving force required to overcome the crack trapping effect would be larger than the effect of the decrease in the PGIB area. Hence, further variation in t would lead to a change in PGIB structure. In a thick film, the PGIB area is determined by D . For a given material and loading mode, D is quite insensitive to the crystallographic orientation and may be regarded as a material constant [25], which may be attributed to the insensitivity of effective fracture work to the twist misorientation [34]. In a thin film, the PGIB area is geometrically affected. As t decreases, the required fracture work to separate the grain boundary is lowered, and vice versa. Thus, the boundary fracture resistance is size dependent (Fig. 3). When the film thickness becomes sufficiently large, this size effect should disappear [25].

Altogether, four groups of thin-film samples were investigated. In each sample, along the grain boundary there is only one BTP. In the same group, all the samples are sliced from the same pre-cracked bicrystal. Thus, they are of the same crystallographic orientation. Clearly, K_{gb} increases with t . For instance, for group 1 samples, the fracture toughness of the grain boundary increases by about 20% as t rises from 2.4 to 12.5 μm . For group 2 samples, as the film thickness increases from 3–4 μm to about 10 μm , the boundary toughness increases by nearly 30%. The data of group 4 samples show that when the film thickness is larger than 20 μm , the grain boundary toughness is size independent, which is typical behavior of thick films. According to data from the literature [12–14], the fracture toughness of a crystallographic plane of single-crystal silicon is about 0.9–1.1 $\text{MPa m}^{1/2}$, nearly 40% smaller than the measured thick-film boundary toughness. Through Eq. (1), the value of C can be determined as 3.4. Note that, since the crystalline structures of the silicon sample are nearly perfect, at the small length scale of the current study, the size dependence caused by the weakest-link effect should be negligible. Even if the weakest-link effect were detectable, it should cause a decrease in K_{gb} as the film becomes thicker. As t rises, the increase in K_{gb} directly reflects the PGIB effect.

The size sensitivity of fracture toughness of group 1 samples is weaker than that of the other three groups, which may be attributed to their crystallographic misorientation angles, especially the twist angle, being the smallest (Fig. 3). When the twist angle is small, as the film thickness varies, the change in PGIB area is less pronounced, and thus the associated variation in the work needed for fracture to occur is less evident. Note that, even though the twist angles of groups 2, 3 and 4 are quite different, their K_{gb} - t relationships are somewhat similar, indicating that as the twist angle exceeds a critical range, the PGIB area is sufficiently large so that direct shear separation is difficult. The crack front first penetrates across the boundary and propagates forward in grain “A”. The PGIB area is left behind the

advancing front, acting as a tough reinforcement bridging the fracture flanks together [27]. Consequently, the criteria of unstable crack growth in grain “A” is not directly dependent on θ . Because mixed-mode fracture is unfavorable, the critical range of twist angle should be relatively small.

To summarize, as the film thickness is relatively small, the grain boundary toughness is no longer a material constant, primarily due to the geometrically affected formation of persistent grain boundary islands. As the thickness is reduced, the toughness may decrease, which must be taken into consideration in micro/nano-fabrication.

This work was supported by the US Department of Energy, Office of Basic Energy Sciences under contract DE-FG02-07ER46355.

- [1] R.A.M. Receveur, F.W. Lindemans, N.F. De Rooij, J. Micromech. Microeng. 17 (2007) R50.
- [2] N.C. Tsai, C.Y. Sue, Sens. Actuators, A 134 (2007) 555.
- [3] A.S. Argon, B.J. Gally, Scripta Mater. 45 (2001) 1287.
- [4] B.J. Gally, A.S. Argon, Philos. Mag. 81 (2001) 699.
- [5] Y. Qiao, A.S. Argon, Mech. Mater. 35 (2003) 903.
- [6] G. Xu, A.S. Argon, M. Ortiz, Philos. Mag. 72 (1995) 415.
- [7] G. Xu, A.S. Argon, M. Ortiz, Philos. Mag. 75 (1997) 341.
- [8] J. Chen, Y. Qiao, Scripta Mater. 56 (2007) 1027.
- [9] H. Kahn, A.H. Heuer, R. Ballarini, MRS Bull. 26 (2001) 300.
- [10] B.D. Jensen, M.P. De Boer, N.D. Masters, F. Bitsie, D.A. LaVan, J. MEMS 10 (2001) 336.
- [11] W.N. Sharpe, B. Yuan, R.L. Edwards, J. Micromech. Microeng. 6 (1997) 193.
- [12] W.N. Sharpe, K.M. Jackson, K.J. Hemker, Z. Xie, J. Micromech. Microeng. 8 (1998) 317.
- [13] S. Greek, F. Ericson, S. Johansson, J. Schweitz, Thin Solid Films 292 (1997) 247.
- [14] S. Greek, F. Ericson, S. Hohansson, M. Furtusch, R. Rump, J. Micromech. Microeng. 9 (1999) 245.
- [15] W.W. van Arsdell, S.B. Brown, IEEE J. MEMS 8 (1999) 319.
- [16] U. Beerschwinger, T. Albrecht, D. Mathieson, R.L. Reuben, S.J. Yang, M. Taghizadeh, Wear 181 (1995) 426.
- [17] U. Beerschwinger, D. Mathieson, R. Reuben, S.J. Yang, J. Micromech. Microeng. 4 (1994) 95.
- [18] I. Chasiotis, S.W. Cho, K. Jonnalagadda, J. Appl. Mech. – Trans. ASME 73 (2006) 714.
- [19] A. McCarty, I. Chasiotis, Thin Solid Films 515 (2007) 3267.
- [20] F.A. McClintock, A.S. Argon, Mechanical Behaviors of Materials, CBL, (1993).
- [21] Y. Ding, C.Q. Wang, Y.H. Tian, B.B. Zhang, Metall. Mater. Trans. A 37 (2006) 1017.
- [22] J.D. Clayton, Theor. Appl. Fract. Mech. 45 (2006) 163.
- [23] S. Kotrechko, B. Strnadel, I. Dlouhy, Theor. Appl. Fract. Mech. 47 (2007) 171.
- [24] Y. Qiao, A.S. Argon, Mech. Mater. 35 (2003) 129.
- [25] Y. Qiao, A.S. Argon, Mech. Mater. 35 (2003) 313.
- [26] D.J. Srolovitz, J. Vac. Sci. Technol., A 4 (1986) 2925.
- [27] Y. Qiao, X. Kong, Mech. Mater. 39 (2007) 746.
- [28] O.M. Jadaan, N.N. Nemeth, J. Bagdahn, W.N. Sharpe, J. Mater. Sci. 38 (2003) 4087.
- [29] Y. Qiao, E. Pan, S.S. Chakravarthula, F. Han, J. Liang, S. Gudlavalleti, J. Mater. Sci. – Mater. Med. 16 (2005) 183.
- [30] K. Hellan, Introduction to Fracture Mechanics, McGraw-Hill, 1984.
- [31] X. Kong, Y. Qiao, Fatigue Fract. Eng. Mater. Struct. 28 (2005) 753.
- [32] G. Michot, Crystallogr. Prop. Prep. 17 (1988) 55.
- [33] J. Chen, Y. Qiao, Scripta Mater. 57 (2007) 1069.
- [34] Y. Qiao, J. Chen, Comput. Mater. Sci., in press.